Hydrotreatment of pyrolytic lignins to aromatics and phenolics using heterogeneous catalysts

Figueirêdo, M. B.; Jotic, Z.; Deuss, P. J.; Venderbosch, R. H.; Heeres, H. J.

Published in:
Fuel processing technology

DOI:
10.1016/j.fuproc.2019.02.020

Publication date:
2019

Fuel Processing Technology 189 (2019) 28–38

Contents lists available at ScienceDirect

Fuel Processing Technology

journal homepage: www.elsevier.com/locate/fuproc

Research article

Hydrotreatment of pyrolytic lignins to aromatics and phenolics using heterogeneous catalysts

M.B. Figueirêdo[a], Z. Jotic[a], P.J. Deuss[a], R.H. Venderbosch[b], H.J. Heeres[a,*]

[a] Department of Chemical Engineering, ENTEG, University of Groningen, Nijenborgh 4, 9747 AG, Groningen, the Netherlands
[b] Biomass Technology Group BV, Josink Esweg 34, 7545 PN Enschede, the Netherlands

ARTICLE INFO

Keywords:
Pyrolytic lignin
Catalytic hydrotreatment
Heterogeneous catalysts
Biobased chemicals

ABSTRACT

The pyrolysis of lignocellulosic biomass generates a liquid product, known as pyrolysis oil, that can be further processed into biofuels and value-added chemicals. During pyrolysis, cellulose and hemicelulose fractions are converted into a range of water-soluble sugar derivatives, for which several valorisation strategies exist. On the other hand, lignin is broken down into so-called pyrolytic lignin, a water-insoluble complex mixture of aromatic oligomers that requires different upgrading strategies than the sugar rich fraction. Here, we report an experimental study on the valorisation of pyrolytic lignin *via* catalytic hydrotreatment in the absence of an external solvent. A variety of carbon-supported noble-metal heterogeneous catalysts were tested (Ru/C, Pd/C, Pt/C and Rh/C), as well as conventional hydrotreatment catalysts (sulphided $NiMo/Al_2O_3$ and $CoMo/Al_2O_3$) to obtain valuable low molecular weight aromatic and phenolic compounds. Overall, depolymerized liquids were obtained with organic yields of up to 63 wt%. Pd/C was shown to be the best catalyst, yielding 59 wt% of monomers based on the organic product (*i.e.* 33 wt% based on pyrolytic lignin intake). While noble metal catalysts favored higher monomer yields, though with some over-reduction of aromatic rings to saturated hydrocarbons, sulphided catalysts were more efficient in deoxygenation and aromatization reactions, but yielded less monomers. The hydrocracking efficiency was shown to be strongly dependent on the reaction temperature. Based on the experimental data, a global reaction network is proposed. The high monomer yields reveal the potential of catalytic hydrotreatment for the upgrading of pyrolytic lignin into valuable phenolics and aromatics.

1. Introduction

Environmental concerns and the need for sustainable solutions for the production of bioenergy, biofuels, biobased chemicals and materials have intensified research related to the valorisation of renewable feedstocks. Lignocellulosic biomass is readily available and as such has been identified as an attractive feedstock for these products. Among the well-established primary technologies for biomass conversion [1], fast pyrolysis stands out as a relatively inexpensive and simple process to liquefy biomass. It yields up to 70 wt% [2] of so-called pyrolysis liquid [3]. Pyrolysis liquids can be further processed either as a whole, or after separation into a sugar and lignin fraction through a simple water fractionation [4]. This fractionation leads to the precipitation of the lignin-derived insoluble fraction, *i.e.* pyrolytic lignin (PL). Since PL and the water-soluble carbohydrate fraction present remarkably distinct characteristics, it enables the separate upgrading of the fractions through specific and more efficient strategies.

Significant structural differences between natural lignins and PLs exist as the harsh conditions applied during pyrolysis cause thermally-driven depolymerization and the formation of new inter-unit C—C linkages in the PLs [5]. These new linkages are much stronger and thus more difficult to break when compared to the ether bonds, typically present in high amounts in native lignins. In order to fully exploit the potential of PLs and to overcome its chemical heterogeneity, further depolymerisation and oxygen removal is required. Catalytic hydrotreatment is one of the most efficient strategies for the valorisation of pyrolysis feedstocks, in which depolymerisation by hydrocracking occurs combined with hydro(deoxy)genation of oxygenated fragments and the formation of water [6]. Despite the extensive amount of literature available for the hydrotreatment of pyrolysis oils, *i.e.* single and multistep approaches [7,8], operation in continuous set-ups [9–11] and exploratory catalyst studies [12–15], upgrading of the individual PL fraction is hardly explored. The aromatic structure of PLs can be converted to a variety of valuable chemicals such as low molecular weight aromatic and phenolic compounds, with applications ranging from transportation fuel (additives), monomers for polymer production and

* Corresponding author.
E-mail address: h.j.heeres@rug.nl (H.J. Heeres).

https://doi.org/10.1016/j.fuproc.2019.02.020
Received 3 January 2019; Received in revised form 17 February 2019; Accepted 22 February 2019

for the preparation of advanced materials.

Early studies report on the hydrotreatment of PLs over HZSM-5 using continuous downflow single and dual reactor systems, tetralin as hydrogen donor and temperatures ranging between 340 and 450 °C under atmospheric pressure [16,17]. Extensive charring was observed, and the amount of organic distillates varied from a maximum of 25 wt% for the single reactor system to 31 wt% for the dual reactor system. No attempt was made to recover tetralin and the reaction products thereof (*e.g.* naphthalene) from the products. Similar low distillate yields were observed on the solvent-free hydrotreatment of PL with a CoMo catalyst in a non-isothermal plug flow reactor with temperatures varying between 240 and 410 °C and 140 bar [18]. PL hydrogenation studies in supercritical ethanol showed that most of the feed was converted into stable organic compounds such as phenols, guaiacols, anisoles, esters, light ketones, alcohols and long-chain alkanes [19]. High loadings of Ru-based catalysts and dilution factors of around 10 were applied, as well as long reaction times. In another study [19], PL was hydrotreated at low temperatures ranging from 25 to 150 °C with ethanol as solvent and high loadings of Ru/TiO_2, leading to the reduction of aromatic rings and low yields of distillates (maximum of 16.3 wt%). A recent study from our group [20] evaluated the solvent-free hydrotreatment of two different PLs at 400 °C and 100 bar, catalyzed by Ru/C. Organic phases were obtained in promising yields of up to 75 wt%, with lowered oxygen contents and large amounts of relatively apolar organics compared to the original PL feed.

Results from previous studies illustrate the potential of catalytic hydrotreatment as a valorisation route for PL. However, the process still presents challenges due to reduced carbon yields by char and gas formation. In addition, the use of a solvent, as commonly used, adds complexity and the need for additional separation steps that significantly impact the operational costs. The identification of active catalysts able to efficiently deoxygenate and depolymerise such complex mixture to added-value products is key for the development of a techno-economically feasible process for PLs suitable to be applied in pyrolysis liquid biorefinery concepts [21].

We here report a systematic catalyst screening study in a batch reactor set-up to evaluate the catalytic hydrotreatment of a pine-derived PL in the absence of an external solvent. In this concept, the original PL serves as the solvent, in a later phase supplemented by low molecular weight reaction products. A variety of carbon-supported noble-metal heterogeneous catalysts were tested (Ru/C, Pd/C, Pt/C and Rh/C), as well as typical hydrotreatment catalysts (sulphided $NiMo/Al_2O_3$ and $CoMo/Al_2O_3$). Reactions were carried out for 4 h, with temperatures in the range of 350–400 °C and 100 bar of hydrogen pressure. Detailed product analyses were performed to determine the extent of depolymerisation, the amounts of the target low molecular weight aromatics and alkylphenolics and the chemical transformations occurring during the catalytic treatment. Finally, a reaction network is proposed to rationalise the experimental findings.

2. Materials and methods

2.1. Chemicals

PL was supplied by Biomass Technology Group (BTG, Enschede, The Netherlands) and obtained by adding water to pine-derived pyrolysis liquids (oil:water ratio of 2:1 on volume basis). The two liquid layers were separated and the water-insoluble bottom layer (PL enriched, typical yield of 25–30 wt%) was used for the experiments. Relevant properties of PL are provided in Table 1. Additional characterization details are given in the Supplementary Information. The noble-metal catalysts Ru/C (d_p = 122 μm by SEM), Pd/C (d_p = 125 μm by SEM), Rh/C (d_p = 139 μm by SEM) and Pt/C (d_p = 108 μm by SEM) were obtained as powders from Sigma Aldrich and contained 5 wt% of active metal. $NiMo/Al_2O_3$ (ref. KF-848, d_p = 268 μm by SEM) and $CoMo/Al_2O_3$ (ref. KF-752, d_p = 235 μm by SEM) were supplied as pellets by Albemarle and crushed before use. Dimethyl disulfide (DMDS) from Sigma Aldrich was used as the sulphur source to activate the catalysts. Nitrogen and helium were obtained from Linde and were all of analytical grade (> 99.99% purity). Tetrahydrofuran (THF), di-n-butyl ether (DBE) and dimethyl sulfoxide (DMSO) were purchased from Sigma-Aldrich. All chemicals in this study were used as received.

Table 1
Relevant properties of the PL used in this study.

Property	Value
Water content (wt%)	4.68
Residual sugar content (wt%, dry basis)[a]	4.98
Elemental composition (wt%, dry basis)	
C	65.9
H	6.48
O	27.5
N	< 0.01

[a] Levoglucosan and glycoaldehyde, estimated via HPLC analysis.

2.2. Catalyst characterization

The surface morphologies and particle sizes of all fresh catalysts were analyzed using scanning electronic microscopy (SEM). Analyses were performed in a FEI Helios G4 CX dual beam workstation with an acceleration voltage of 5 kV and magnifications ranging from 100 to 20,000×.

Average metal nanoparticle sizes of the carbon-supported catalysts were determined experimentally by transmission electronic microscopy (TEM) analyses, and the results are reported in Table 2 (see Fig. S1 for the TEM images). TEM analyses were performed with a Philips CM12 (acceleration voltage of 120 kV). The samples were ultrasonically dispersed in ethanol and subsequently deposited on a mica grid coated with carbon before measurement.

2.3. Catalytic hydrotreatment experiments

PL was hydrotreated in a 100 mL batch autoclave (Parr), with maximum pressure and temperature of 350 bar and 500 °C. The reactor was surrounded by a metal block containing electrical heating elements and channels allowing the flow of cooling water. The reactor content was stirred mechanically at 1000 rpm using a Rushton type turbine with a gas induced impeller. This stirring speed was selected based on previous studies on the catalytic hydrotreatment of lignins and pyrolysis oils. In a typical experiment, the reactor was charged with 15 g of PL and 0.75 g (*i.e.* 5 wt% on PL intake) of catalyst. In the case of the sulphided catalysts (*i.e.* $NiMo/Al_2O_3$ and $CoMo/Al_2O_3$) around 0.38 g (*i.e.* 2.5 wt% on PL intake) of dimethyl sulfide (DMDS) was added. Subsequently, the reactor was pressurized to 120 bar with hydrogen at room temperature for leak testing, flushed three times and pressurized again to 100 bar. The reactor was heated to the desired temperature at a heating rate of around 10 °C min^{-1}, and the reaction time was set at zero when the pre-determined temperature was reached. After the pre-determined reaction time of 4 h, the reactor was cooled to room temperature at a rate of about 40 °C min^{-1}. The final pressure was recorded for mass balance calculations, and the gas phase was sampled in a gas bag to analyze the gas composition. The liquid product was collected

Table 2
Average metal nanoparticle size for the catalysts used in this study.

Catalyst	Average metal nanoparticle size (nm)
Ru/C	2.2
Pd/C	3.4
Pt/C	2.3
Rh/C	4.1

and weighed. In all cases it consisted of two layers: an organic product layer and an aqueous layer, which were separated by decantation, allowing the quantification and analysis of each phase separately. Char formation was not observed. However, to gain insights in the amount of organics deposited on the catalyst surface, the spent catalyst was washed with acetone, followed by drying and gravimetric analysis. The organic product layer was further analyzed by various spectroscopic, chromatographic and wet-chemistry techniques. All experiments were carried out in duplicate. The relative experimental error for each sample was calculated by dividing the standard deviation by the average value multiplied by 100%.

2.4. Liquid product analyses

The liquid products were analyzed using a number of techniques, among others the average molecular weight and molecular weight distribution (GPC), charring tendency (TGA), water content, elemental composition (CHO analyses), monomeric yield/identification (GCxGC, GC/MS-FID) and structural features (NMR).

GPC analyses of the feed and products were performed using an Agilent HPLC 1100 system equipped with a refractive index detector. Three columns in series of MIXED type E (length 300 mm, i.d. 7.5 mm) were used. Polystyrene standards were used for calibration. 0.05 g of the sample was dissolved in 4 mL of THF together with 2 drops of toluene as the external reference and filtered (filter pore size 0.45 μm) before injection.

GCxGC-FID analyses were performed on a trace GCxGC system from Interscience equipped with a cryogenic trap and two capillary columns, *i.e.* a RTX-1701 capillary column (30 m × 0.25 mm i.d. and 0.25 μm film thickness) connected by a Meltfit to a Rxi-5Sil MS column (120 cm × 0.15 mm i.d. and 0.15 μm film thickness) and a flame ionization detector (FID). The injector temperature was set to 280 °C. A dual jet modulator was applied using carbon dioxide to trap the samples after passing through the first column. Helium was used as the carrier gas (continuous flow rate of 0.8 mL/min). The oven temperature was kept for 5 min at 40 °C and then increased to 250 °C at a rate of 3 °C min^{-1}. The pressure was set at 0.7 bar at 40 °C and the modulation time was of 6 s. Quantification of GCxGC main groups of compounds (*e.g.* aromatics, alkanes, alkylphenolics) was performed by using an average relative response factor (RRF) per component group in relation to an internal standard (di-n-butyl ether, DBE). All samples were diluted around 25 times with a 500 ppm solution of DBE in THF.

Heteronuclear single quantum coherence (HSQC) NMR spectra were recorded by a Varian Unity Plus (400 MHz) with the following parameters: 11 ppm sweep width in F_2 (1H), 220 ppm sweep width in F_1 (^{13}C), 8 scans, 1024 increments and a total acquisition time of around 6 h. Sample preparation involved the dissolution of 0.35 g of sample with 0.35 g of dmso-d_6.

^{13}C NMR spectra were acquired on a Bruker NMR spectrometer (600 MHz) using a 90° pulse and an inverse-gated decoupling sequence with relaxation delay of 5 s, sweep width of 220 ppm and 2048 scans, with a total acquisition time of 3.5 h and TMS as reference. Sample preparation involved the dissolution of 0.35 g of sample in 0.35 g of dmso-d_6.

Gas chromatography/mass spectrometry (GC/MS-FID) analyses were performed on a Hewlett-Packard 5890 gas chromatograph equipped with a RTX-1701 capillary column (30 m × 0.25 mm i.d. and 0.25 μm film thickness) and a Quadrupole Hewlett-Packard 6890 MSD selective detector attached. A split ratio of 1:25 was applied. Helium was used as carrier gas (flow of 2 mL/min). The injector and FID temperatures were set to 280 °C. The oven temperature was kept at 40 °C for 5 min, then increased to 250 °C at a rate of 3 °C min^{-1} and held at 250 °C for 10 min. Quantification of main groups of compounds (*e.g.* aromatics, alkanes, alkylphenolics) was performed by using an average relative response factor (RRF) per component group in relation to an internal standard (di-n-butyl ether, DBE). All samples were diluted around 25 times with a 500 ppm solution of DBE in THF.

The water content was determined by Karl Fischer titration using a Metrohm 702 SM Titrino titration device. About 0.01 g of sample was injected in an isolated glass chamber containing Hydranal (Karl Fischer solvent, Riedel de Haen). The titrations were carried out using the Karl Fischer titrant Composit 5 K (Riedel de Haen). All analyses were performed at least 3 times and the average value is reported.

Elemental analysis (C, H, N) was performed using a EuroVector EA3400 Series CHNS-O analyzer with acetanilide as the reference. The oxygen content was determined indirectly by difference. All analyses were carried out at least in duplicate and the average value is reported.

Principal component analyses (PCA) were performed in Python (version 3.7) using the Scikit-learn (version 0.19) module.

2.5. Gas phase analysis

The gas phases were collected in a gas bag (SKC Tedlar 3 L sample bag (9.5″ × 10″)) with a polypropylene septum fitting. GC-TCD analyses were performed using a Hewlett Packard 5890 Series II GC equipped with a Porablot Q Al_2O_3/Na_2SO_4 column and a molecular sieve (5 A) column. The injector temperature was set at 150 °C and the detector temperature at 90 °C. The oven temperature was kept at 40 °C for 2 min then heated up to 90 °C at 20 °C min^{-1} and kept at this temperature for 2 min. A reference gas (containing 55.19% H_2, 19.70% CH_4, 3.00% CO, 18.10% CO_2, 0.51% ethylene, 1.49% ethane, 0.51% propylene and 1.50% propane) was used to quantify the gaseous products.

3. Results and discussion

3.1. Catalysts and screening conditions

Four noble-metal catalysts (Ru, Pt, Pd and Rh supported in carbon, all containing 5 wt% of metal loading) and two typical hydrotreatment catalysts ($NiMo/Al_2O_3$ and $CoMo/Al_2O_3$) were selected for the screening experiments using PL as feedstock. Noble-metal catalysts are known to be very reactive in the hydrotreatment of pyrolysis liquids [7,12,15]. The reactions were conducted at a temperature range of 350–400 °C and 100 bar for 4 h. These conditions were selected on basis of earlier research performed in our group [12]. The best catalysts at 350 °C (*i.e.* $NiMo/Al_2O_3$ and Pd/C) as well as the Ru/C benchmark catalysts were further evaluated at more severe conditions (375 and 400 °C). To reduce complexity and costs, no additional solvents were applied. As such, the PL feed, a viscous liquid at room temperature containing residual sugars and moisture (Table 1), acts both as solvent and reactant.

All experiments were carried out in duplicate. A blank experiment (without catalyst and at 350 °C) was also performed to investigate the extent of thermal depolymerisation, and produced only 3 wt% of an oil after reaction together with large amounts of char (64.4 wt%). As such, an efficient catalyst to achieve satisfactory oil yields with improved product properties is required.

3.2. Catalytic hydrotreatment of PL

For all experiments, a liquid phase consisting of two immiscible layers, *i.e.* a top dark brown organic phase and a clear aqueous bottom phase was obtained after reaction. The formation of water is indicative for the occurrence of hydrodeoxygenation reactions. Solids formation was overall negligible, being opposed to results reported in literature for the hydrotreatment of pyrolysis liquids. This suggests that the formation of solids is strongly related to the sugar fraction, as also stated in recent studies [7,27]. Nevertheless, some deposition of organics on the catalyst surface was observed by washing the catalyst after reaction with acetone. The data are given in Fig. 1, showing that these amounts are at maximum 4.8 wt% (based on PL intake for NiMo at 400 °C) and in

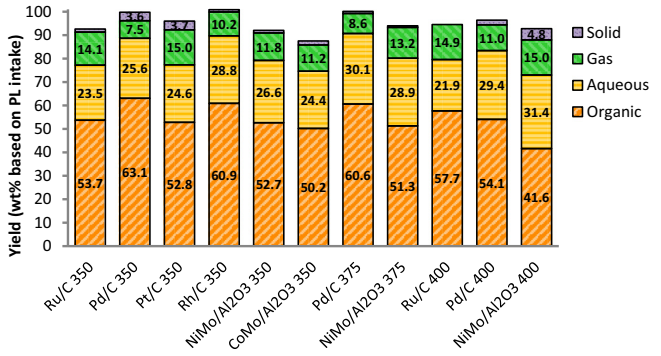

Fig. 1. Product yields for the catalytic hydrotreatment of PL with different catalysts and process conditions.

most cases by far lower. Confirmation of deposition of organics on the catalyst was obtained from TGA measurements for fresh and used Pd/C (see Fig. S4). For instance, the mass loss between 30 and 350 °C (*i.e.* the temperature range in which the carbon support is stable) increased from 5.8 wt% in the fresh Pd/C (mostly due to water) to 20.8 wt% (350 °C reaction) and 13 wt% (400 °C reaction). Such deposits can lead to catalyst deactivation due to blockage of the active sites and impact its reusability, being a known bottleneck on pyrolysis liquids hydroprocessing [14].

The organic phases were obtained in yields up to 63.1 wt% based on PL intake (Fig. 1). The oxygen contents of the product oils were considerably lower than for the PL feed, with the largest oxygen reduction for the oil obtained with $NiMo/Al_2O_3$ (see Table 3). The organic phases contained large amounts of carbon (> 81 wt% on dry basis) and limited amounts of dissolved water (0.3–3.0 wt%). Higher reaction temperatures led to lower organic yields and higher amounts of gas and aqueous phase, which is explained by the higher catalyst activity for both hydrodeoxygenation and hydrocracking pathways.

When considering the product yields, Pd/C gave the best performance, *i.e.* highest organic yields and lowest amounts of gas and solids deposited on the catalyst. These aspects are of high relevance to minimize carbon losses. The average mass balances, carbon balances, carbon yields for the organic products and elemental analysis results for the organic products (wt% dry) are reported in Table 3. Good mass balance closures (mostly higher than 90%) were observed. Quantification of the amounts of aqueous phases was cumbersome due to experimental separation issues.

Table 3
Mass/carbon balances and elemental analysis for the organic products.

Temperature °C	Catalyst	Mass balance	Carbon balance	Carbon yield[a]	C (wt % dry)	H (wt % dry)	O (wt % dry)
350	Ru/C	89.6	83	70.8	82.9	9.8	7.2
	Pd/C	96.8	91.8	81	80.7	9.5	9.8
	Pt/C	93	85.2	70.8	84.3	10.7	5.0
	Rh/C	98.2	87.3	78.9	81.5	9.3	9.2
	NiMo/Al	88.4	82.6	71.6	85.7	10.1	4.1
	CoMo/Al	84.4	80.3	68.5	84.9	8.9	6.2
375	Pd/C	96.5	87.9	79.7	82.6	10.3	7.1
	NiMo/Al	90.1	81.7	70.2	86.0	9.8	4.2
400	Ru/C	90.8	89.4	77.1	84.1	9.5	6.4
	Pd/C	93	82.9	70.9	82.4	10.1	7.5
	NiMo/Al	89.1	77.5	57.7	87.2	8.6	4.2
		2.97	1.98	2.88	0.1	0.4	2.7

[a] Yield (wt%) of carbon in the organic products.

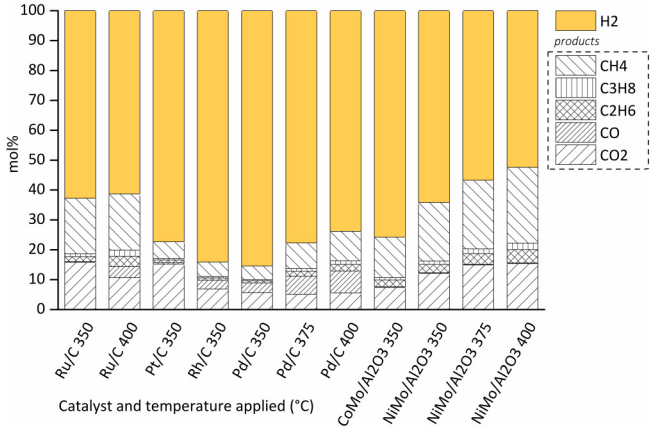

Fig. 2. Gas phase composition after the catalytic hydrotreatment of PL.

3.3. Composition of the gas and liquid phases

3.3.1. Gas phase composition

The gas phase composition after reaction is a strong function of the catalyst used (see Fig. 2). Over 50 mol% corresponded to unconverted H_2, indicating that all reactions were carried at an excess of hydrogen. The main identified gaseous products were CH_4, CO and CO_2, along with smaller amounts of C_2-C_3 hydrocarbons resulting from catalytic hydrocracking reactions. With respect to carbon losses to the gas phase, CH_4 and CO_2 are the main contributors (see Fig. 2 and Fig. S5). In addition, carbon losses to gaseous hydrocarbons increases at higher temperatures, likely due to hydrocracking reactions (*vide infra*).

Carbon dioxide and carbon monoxide (CO_2 and CO) are commonly formed by acid-catalyzed decarboxylation and decarbonylation reactions of reactive lignin fragments. CO can be also derived from the reverse water-gas shift (RWGS) reaction, which is known be kinetically favored when using noble metal catalysts [22]. This is evident when observing both the results of Pd/C and Ru/C, in which the amount of CO increases when increasing the reaction temperature.

Methane (CH_4) is likely produced by methanation of CO and/or CO_2 (see Eqs. (1) and (2)), but possibly also directly from the hydrogenolysis of methoxy substituents present on the aromatic network of PLs (see Eq. (3)). This reaction was shown to occur during model reactions of anisole and guaiacol with hydrogen using a NiMo on SiO_2–Al_2O_3 catalyst at 250–350 °C [23]. Indeed, PL contains significant amounts of methoxy groups [24,25], supported by NMR analyses presented in this work (*vide infra*).

$$CO + 3H_2 \leftrightarrow CH_4 + H_2O \quad (1)$$

$$CO_2 + 4H_2 \leftrightarrow CH_4 + 2H_2O \quad (2)$$

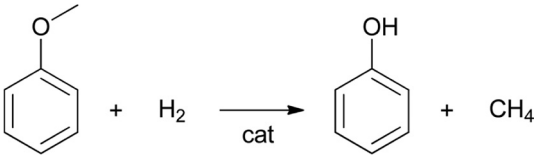

(3)

Methanation is known to be catalyzed by supported Ru catalysts [7,12]. The relatively lower final hydrogen concentration and higher methane production observed in the gaseous products for the reactions catalyzed by Ru/C (Fig. 2) are in accordance with this statement.

Pd/C showed the lowest amounts of gas phase components after reaction, with minor amounts of CO, CO_2 and CH_4, suggesting that hydrogen was mostly consumed for the hydrocracking and hydrodeoxygenation reactions. Apparently Pd/C is relatively more selective towards the desired reactions, an important observation in terms of process feasibility due to the high costs associated with hydrogen consumption.

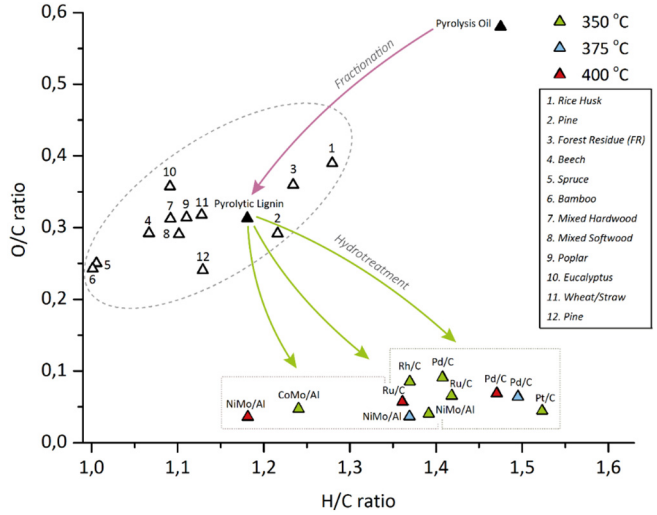

Fig. 3. Van Krevelen plot of the PL feed, hydrotreatment products and relevant literature data.

3.3.2. Liquid phase composition and properties

The elemental composition of feed and hydrotreated oils are given in Fig. 3 in the form of a van Krevelen plot (O/C *versus* the H/C molar ratios). For comparison, literature data on the elemental composition of PLs from different sources are also plotted [20,24,26,27]. The elemental composition of the various PLs covers a wide range of H/C and O/C ratios (*i.e.* 0.2–0.4 for O/C and 1.0–1.3 for H/C), implying that the PL structure varies considerably. This could be due to differences in the biomass source and on the extraction procedure. The pine-derived PL used in this study has an intermediate H/C and O/C ratios (1.17; 0.31). A data point corresponding to the pine-derived pyrolysis oil feed is also given. When comparing the data for the pyrolysis oil and the PL, it is clear that the oxygen content is considerably lower for the latter. This is advantageous when aiming for products with low oxygen content by hydrotreatment reactions as it is associated with lower hydrogen consumption [19].

The product oils show considerably lower O/C ratios than the feed (values of below 0.1), whereas the H/C ratios are increased (between 1.2 and 1.5). Interestingly, product oils from sulphided and noble-metal catalysts show different trends at similar hydrotreatment temperatures. The oils of the former catalyst show lower O/C ratio, an indication for a higher activity for deoxygenation reactions. However, the H/C ratios are lower, implying that the sulphided catalysts are less active for hydrogenation reactions of for instance the aromatic rings (*vide infra*) than noble-metal catalysts [28–30].

Of interest is also the effect of temperature on the elemental composition and particularly the H/C ratio of the product oils. For Pd/C, an increase in the temperature led to product oils with higher H/C values, indicating a higher hydrogenation activity (*e.g.* of C—C double bonds) of the catalyst at higher temperatures (Fig. 3). In contrast, the H/C ratio was strongly reduced for the $NiMo/Al_2O_3$ catalyst products with an increase in temperature. This puzzling observation may be due to the occurrence of dehydrogenations reactions leading to *e.g.* aromatics from aliphatic compounds [31]. It is in line with studies with $NiMo/Al_2O_3$ on the hydrotreatment of heavy oils for the production of asphaltenes [32], rationalized by considering that dehydrogenation reactions are thermodynamically favored at higher temperatures. This reduction in H/C ratio at elevated temperature due to aromatics formation is also in line with GCxGC and NMR results (*vide infra*), which show a relatively higher aromatic content for $NiMo/Al_2O_3$ products, especially at higher temperatures.

The oils were analyzed by GC/MS-FID to identify the main molecules formed during catalytic hydrotreatment. A representative chromatogram for products obtained over Pd/C at 400 °C is given in Fig. 4, showing over 300 volatile components in the mixture. Significant amounts of (alkyl substituted) phenolics, aromatics and cyclic alkanes were present. Quantification of the main individual components in the various product classes are given in Table 4, showing that alkylphenolics are present in high amounts. These main components together correspond to around 30.5 wt% of the product oil. The GC spectra of the hydrotreated products differ substantially from the initial PL feed, in which only few peaks related to guaiacols, acetic acid, vanillin and residual sugars are detected (see Fig. S3).

To gain more insights into the various product classes present in the product oils, GCxGC-FID analyses were performed, allowing a better peak separation and quantification of major component classes. A representative chromatogram is given in Fig. 5, including the identification of each component class. A clear separation between the classes can be observed.

Quantification of the various product classes was performed using established procedures [20] and the results are given in Fig. 6. The main GCxGC detectable products in the different product oils were alkylphenolics, followed by aromatics, (cyclo)alkanes and naphtalenes. Overall, noble-metal catalysts provided higher monomeric yields, especially with respect to alkylphenolics, while sulphided catalysts yielded less oxygenated products and relatively more aromatics. These results are in accordance with previous studies that showed a higher activity for $NiMo/Al_2O_3$ and $CoMo/Al_2O_3$ for deoxygenation pathways (*e.g.* dehydration, hydrolysis, decarbonylation, decarboxylation) [33,34], as well as a higher activity of noble metals for reduction of aromatic rings [30,35]. $CoMo/Al_2O_3$ presented the lowest amount of GC-detectables, which is related to a poor hydrocracking performance at the applied temperature. This is in line with the GPC results (*vide infra*), in which the products hydrotreated with $CoMo/Al_2O_3$ presented a relatively high molecular weight (Mw) in comparison with products obtained with the other catalysts at the same temperature (*i.e.* 350 °C).

The effect of reaction temperature on the amount of detected monomers was more prominent for Pd/C and Ru/C in comparison with $NiMo/Al_2O_3$. For instance, while the GCxGC detectables increased by around 50% when increasing the reaction temperature from 350 °C to 400 °C for Pd/C and Ru/C, the overall increase was limited for $NiMo/Al_2O_3$. With respect to the monomers distribution, cycloalkanes were favored at higher temperatures for noble metals, while the proportion of aromatics increased for $NiMo/Al_2O_3$. This observation suggests the occurrence of dehydrogenation reactions, in line with the elemental analysis and NMR data.

The amount of species quantified by the GCxGC-FID technique reached a maximum of 59 wt% (on organic product oil) for Pd/C at 400 °C, corresponding to around 33 wt% of the PL feed being converted to detectable low molecular weight compounds. From this amount, two-thirds consisted of aromatics and phenolics.

Despite the high monomer yields achieved with the catalytic hydrotreatment, still significant amounts of higher molecular weight, non-GC detectables are present. This was confirmed by performing GPC analyses for both the PL feed and hydrotreated products (see Figs. 7 and 8). The molecular weight distributions (weight averaged) of the hydrotreated products are shifted towards lower Mw when compared to the PL feed, indicating that substantial depolymerisation took place during catalytic hydrotreatment. Nonetheless, relatively large fractions corresponding to oligomers can still be observed.

When comparing the results for the various catalysts at 350 °C, the product oils show similar average Mw values (Fig. 8). The only exception is $CoMo/Al_2O_3$, which showed a considerably higher average Mw value and extended tailing. This implies that the CoMo catalyst is less active than the others for depolymerisation by hydrocracking reactions at this temperature. Previous studies [36–40] also indicated the lower activity of CoMo in comparison with NiMo for hydrodeoxygenation and hydrodesulfurization reactions of model compounds, diesel fuel and heavy oils. In addition, a recent study on the solvent-free catalytic hydrotreatment of Kraft lignin [41] also showed a

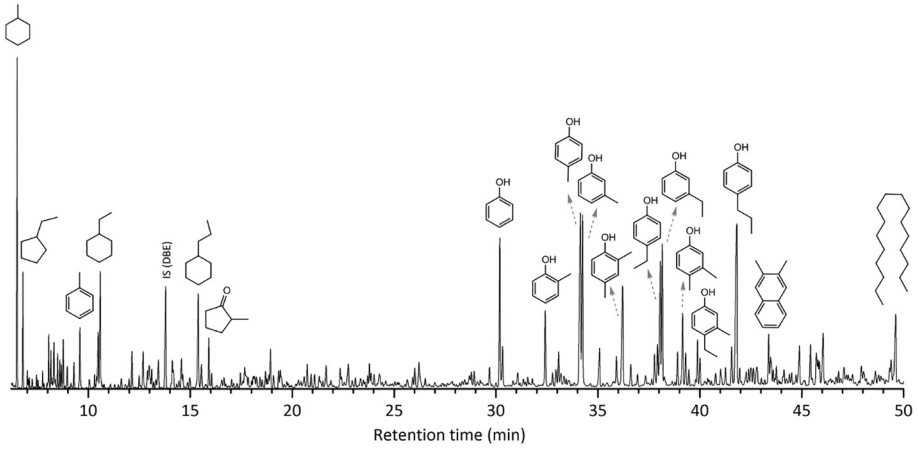

Fig. 4. GC/MS-FID chromatogram of the organic product from a PL hydrotreated with Pd/C.

Table 4
Main groups of compounds detected by GC–MS-FID in the organic phase for a hydrotreatment reaction performed using Pd/C at 400 °C.[a]

Alkylphenolics (wt%)		Aromatics (wt%)		Aliphatics (wt%)	
Phenol	1.8	Toluene	0.7	Hexane	1.1
2-, 3- and 4-methylphenol	6.4	Naphtalene	0.6	Cyclohexane	0.2
3- and 4-ethylphenol	3.6	2,3-Dimethyl naphtalene	0.8	Methyl cyclohexane	2.4
2,4- and 3,4-dimethylphenol	2.8			Ethyl-, propyl-cyclohexane	2.6
4-Propylphenol	3.5			Ethyl-, propyl-cyclopentane	1.5
4-Ethyl-3-methylphenol	0.6			Heptadecane	1.5

[a] wt% based on the organic product oil, values were determined by using a response factor relative to the internal standard (DBE).

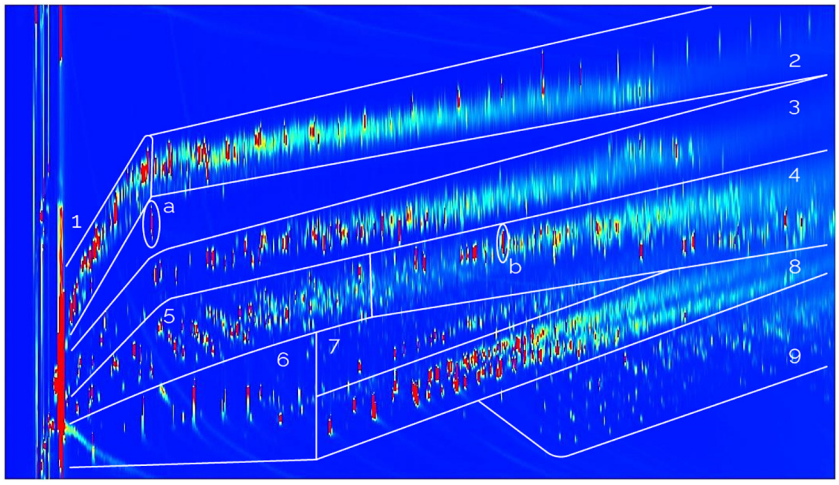

Fig. 5. GCxGC-FID chromatogram of the organic phase after hydrotreatment with Pd/C. 1 = cyclic alkanes, 2 = linear/branched alkanes, 3 = aromatics, 4 = naphtalenes and polycyclic aromatic hydrocarbons, 5 = ketones/alcohols, 6 = acids, 7 = guaiacols, 8 = alkylphenolics, 9 = catechols. Also a = internal standard and b = BHT (stabilizer in THF).

lower monomer yield, thus a lower hydrocracking tendency for sulphided $CoMo/Al_2O_3$ compared to sulphided $NiMo/Al_2O_3$. The MW distributions are clearly dependent on the reaction temperature, and higher temperatures led to a reduction in the molecular weight, indicating that hydrocracking reactions are favored at such higher temperatures.

The volatility of the product oils was determined using TGA analysis (see Supplementary information, Figs. S6–S8). In a typical TGA curve for the PL feed, the weight loss occurs mostly between 100 °C and 500 °C (see Fig. S7), and a residue (*i.e.* non-volatile fraction) of around 27 wt% was observed. Overall, the hydrotreated products presented a significantly higher volatility. In addition, products obtained at 350 °C showed by far lower residue values (2–6 wt%,) than the PL feed, indicating improved thermal stability. The only exception was $CoMo/Al_2O_3$ (16 wt%). This observation is in line with the relatively higher MW and lower monomer yields indicated by GPC and GCxGC analyses of $CoMo/Al_2O_3$ products (*vide supra*), ratifying the lower activity of this catalyst for PL hydrotreatment. Product oils obtained at higher hydrotreatment temperatures (375 °C and 400 °C), from noble-metal catalysts were fully evaporated (100% mass loss, no residue) when the sample temperature in the TGA device was increased from room temperature to 350 °C.

Interestingly, significant difference in TGA profiles was found for the sulphided and non-sulphided catalysts. In general, the products from noble metal catalysts presented higher volatility in comparison with $NiMo/Al_2O_3$. Furthermore, the TGA residue from $NiMo/Al_2O_3$ products was essentially independent of the reaction temperature (see Fig. S8). The TGA trend is in accordance with GCxGC integration results, in which the monomer yields of $NiMo/Al_2O_3$ is not a clear function of the reaction temperature. Accordingly, TGA residue and GCxGC

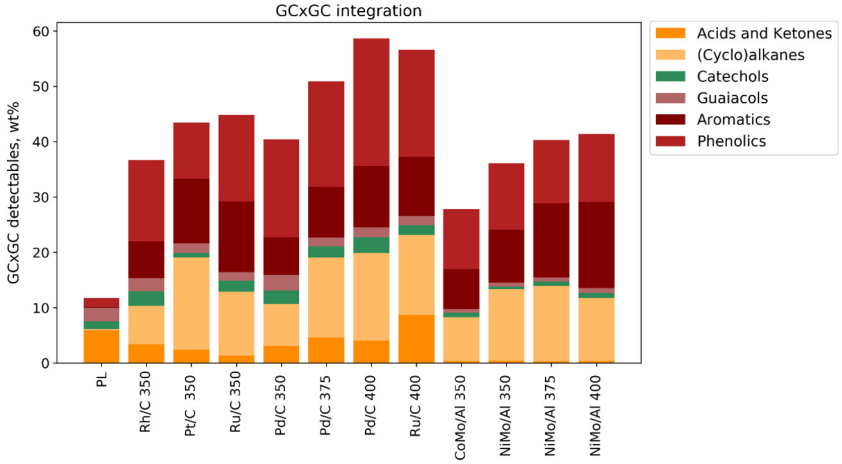

Fig. 6. Composition of the product oils by GCxGC-FID (wt% on organic product oil).

detectables showed a clear (inverse) correlation for all product samples (see Fig. S9), in which high TGA residues relate to low amounts of GCxGC detectables and *vice-versa*.

To get insights in the chemical composition of the product oils including non-volatiles, a 2D-NMR technique was deployed, enabling the identification of main changes in chemical composition of the PL feed and product oils. This information gives valuable insights in the reactions occurring during the hydrotreatment process. Two representative product oils obtained from Pd/C and NiMo/Al_2O_3 catalyzed reactions at 400 °C were selected and compared with the PL feed (see Fig. 9). The spectra can be divided into four main areas, *i.e.* aliphatics, oxygenated aliphatics, aromatics and aldehydes, and semi-quantitative analysis is possible by integrating the signals within a certain peak area. Major changes occur in the area corresponding to oxygenated aliphatic bonds and actually most signals are absent after the hydrotreatment reactions. In addition, the aldehyde signals related mostly to small molecules present in the PL mixture (*e.g.* vanillin) disappear as well. Peak intensities in two areas increased significantly during hydrotreatment, *i.e.* aromatics and aliphatics regions, being in line with the GC results. Furthermore, the presence of high amounts of aromatic components in the product oils from NiMo/Al_2O_3 compared with Pd/C are clearly visible, in line with GCxGC and elemental analyses data. Accordingly, the relative aromatic/aliphatic ratio obtained from the integration of each respective region in the Figure was 0.51 for Pd/C and 0.75 for NiMo/Al_2O_3. The integration results (Fig. S10) show that the sulphided catalysts resulted in product oils with relatively more aromatics compared to oils obtained with noble metal catalysts.

A similar comparison of the NMR HSQC spectra was done for the product oils obtained with NiMo/Al_2O_3 at different temperatures (see Fig. S11). By integrating the main peak areas, a gradual increase of the aromatic area with the reaction temperature was observed, in line with elemental analysis results. For instance, the aromatic/aliphatic ratio of the products increased from 0.48 (350 °C) to 0.75 (400 °C). As such, the NMR data also support the observation that dehydrogenation of aliphatics to aromatics occurs to a significant extent at elevated temperatures.

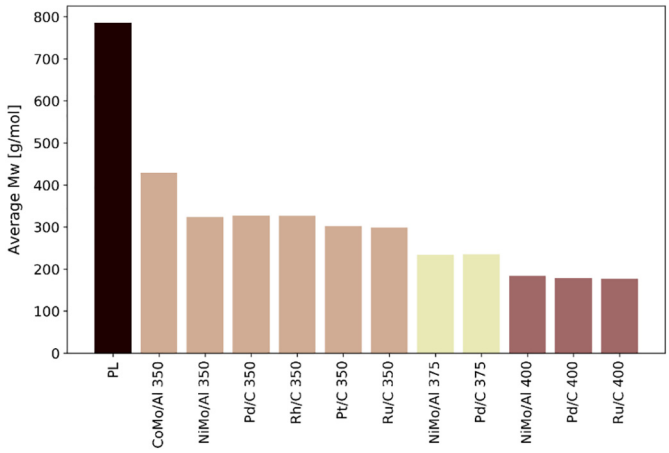

Fig. 8. Average Mw for PL and hydrotreated products.

Additional ^{13}C NMR analyses aided further elucidation of the molecular composition of the hydrotreated oils. Representative ^{13}C NMR spectra of Pd/C and NiMo/Al_2O_3 with the area% for each type of carbon is shown in Fig. 10. The data confirm the higher aromatics content in the product oils obtained using the sulphided catalysts.

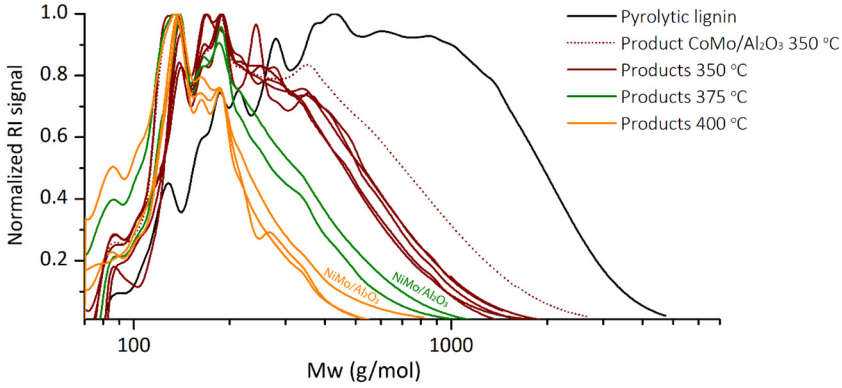

Fig. 7. GPC results for the PL feed and hydrotreated products.

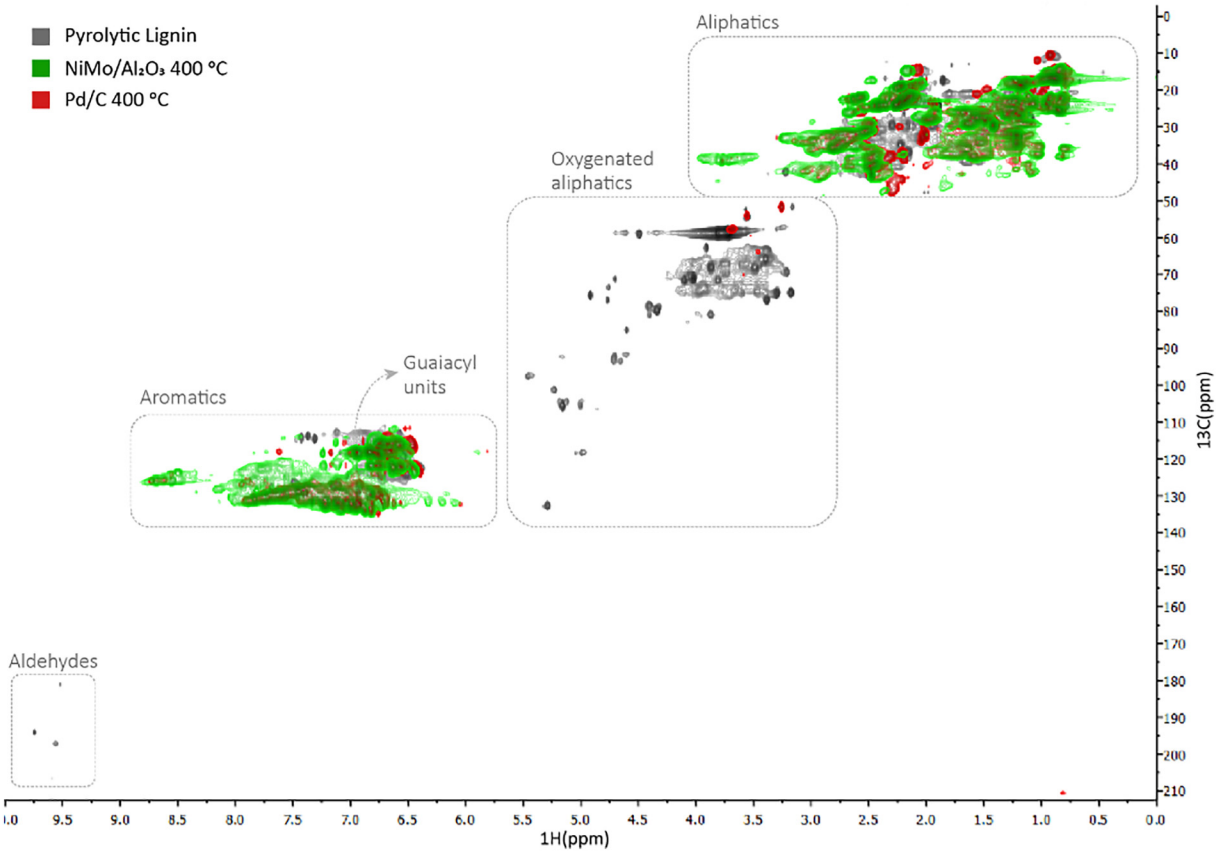

Fig. 9. NMR HSQC spectra of the PL feed and hydrotreated products with Pd/C and NiMo/Al_2O_3.

3.4. Principal component analysis

A number of relevant analytical data of the hydrotreated products (*i.e.* O/C and H/C ratios, GCxGC detectables, average Mw, TGA residue, carbon yields and relative area% from the integration of the 2D-NMR spectra) was used in a principal component analysis (PCA). PCA is a statistical method that allows the dataset to be projected in a lower dimensional space, while retaining most of the information. Accordingly, it determines the directions of maximum variance in the dataset, the so-called principal components (PCs), turning those into a new coordinate system. PCA has been successfully applied to lignin datasets to: *i*) facilitate data visualization and interpretation when having a large number of datapoints; *ii*) identify correlations and variation sources within the datasets; and *iii*) classify lignins according to origin and processing conditions [42–44]. The PCA performed with the present dataset resulted in 83.2% of the total variance explained by the

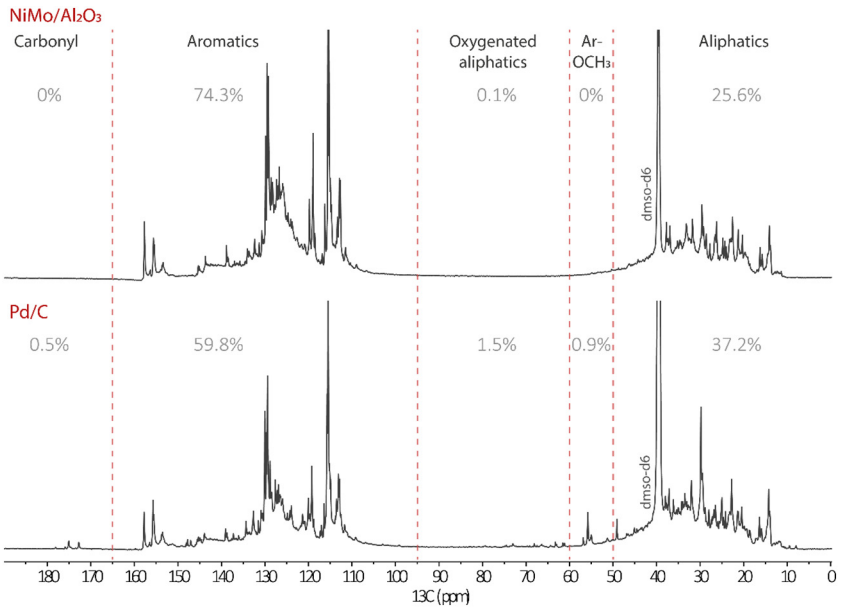

Fig. 10. Comparative ^{13}C NMR spectra of PL hydrotreated with NiMo/Al_2O_3 and Pd/C.

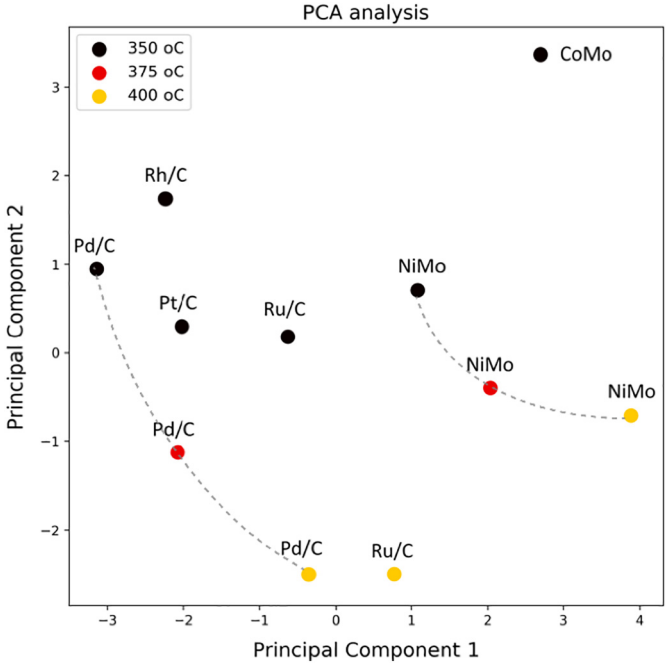

Fig. 11. Score plot (PC1 and PC2) from the PCA of the hydrotreated products.

first two PCs (PC1 = 52.6% and PC2 = 30.6%). Therefore, a score plot of PC1 and PC2 can be reliably used to detect clusters, outliers and trends, as most of the variance in the data is addressed. From the score plot in Fig. 11 follows that the PLs hydrotreated with different catalysts but at the same reaction conditions vary mostly in terms of PC1 (x axis), while the products hydrotreated at different temperatures are clustered according to PC2 (y axis).

For a better understanding of the clustering, the contributions of each variable of the dataset to PC1 and PC2 were further assessed through so-called loadings [42] (see Fig. 12). A higher loading is related to a higher influence of the variable on the respective PC. For instance, PC1 is strongly influenced by the structural characteristics of the oils (*i.e.* 2D-NMR relative areas, H/C and O/C ratios), which indeed varied considerably among the evaluated catalysts due to the differences in deoxygenation levels. The carbon yields also have a large effect on PC1, being likely related to the difference in carbon losses to the gas phase, which is experimentally shown to be a strong function of the catalyst composition (see Fig. 1).

The second principal component, PC2, is related to the hydrocracking extent, being largely influenced by the average Mw, TGA residue and GCxGC detectables. The clustering of products obtained at different reaction temperatures with respect to PC2 confirms that temperature is a parameter of crucial importance for the depolymerization of PL's. Furthermore, the separation between $CoMo/Al_2O_3$ and the other catalysts at 350 °C in terms of PC2 can be explained by its poor hydrocracking performance of the latter as confirmed by GPC, TGA and GCxGC analyses (*vide supra*). When analyzing the score trends of Pd/C and $NiMo/Al_2O_3$ at 350 °C, 375 °C and 400 °C (*i.e.* dashed lines in Fig. 11), it is clear that products obtained by Pd/C show larger variations in terms of PC2, which is expected because of the larger variations in monomer yields and volatility observed at different reaction temperatures (*vide supra*).

3.5. Proposed reaction network

Based on the chemical composition of the gas and liquid products, molecular weight distributions and structural insights provided by NMR of the product oils, a global reaction network is proposed for the catalytic hydrotreatment of PLs (Fig. 13). Within this framework, catalysts play a major role by favoring specific pathways. In non-catalytic runs or in case of low catalyst activity, thermal repolymerisation *via e.g.* condensation reactions (pathway 5) takes place, leading to high molecular weight fragments that can end up in the system as char (pathway 6). Accordingly, the blank reaction produced mainly char and only 3 wt% of a product oil.

For all catalysts studied, the initial step involves the catalytic breakdown of the PL feed to smaller molecular weight fragments by depolymerisation reactions (pathways 1 and 4). The PL structure is, besides some ether linkages, rich in C—C bonds (*e.g.* biphenyl linkages [24,25]) as a result of the thermally-driven reactions occurring during pyrolysis. The cleavage of the latter bonds is key for the catalytic hydrotreatment process [24,25]. As such, the catalysts should possess significant hydrocracking activity. PL depolymerization under the applied conditions is likely a two-step process, in which the ether bonds are initially cleaved followed by the breakdown of more stable C—C bonds.

The lower molecular weight oxygenated aromatics are subsequently converted by catalytic hydrodeoxygenation reactions to aromatics (pathway 2), and further hydrogenated to (cyclic)alkanes (pathway 3). Formation of alkanes may either occur directly from the oxygenated aromatics by hydrogenation of the aromatic C—C double bonds followed by dehydration reactions, and/or by cleavage of the O—C bonds. The exact extent of each specific route cannot be assessed without a detailed product composition–time study. Hydrocracking reactions also

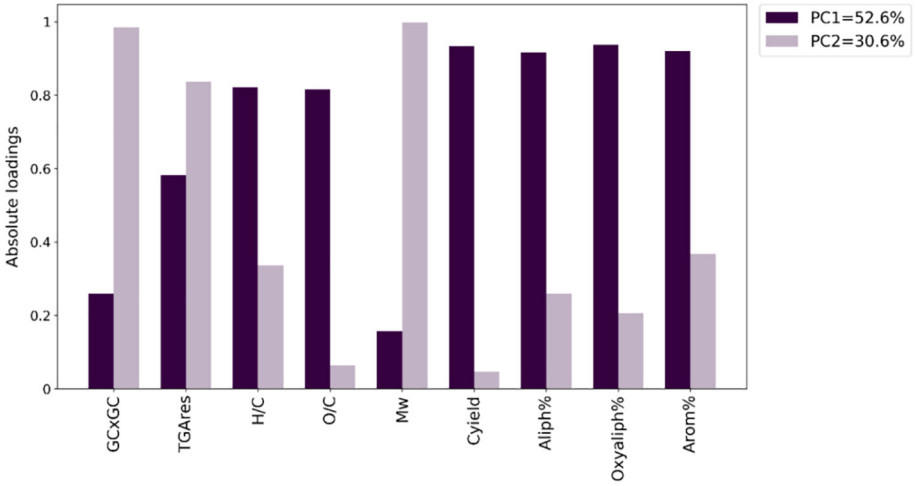

Fig. 12. Contribution of each variable to PC1 and PC2.

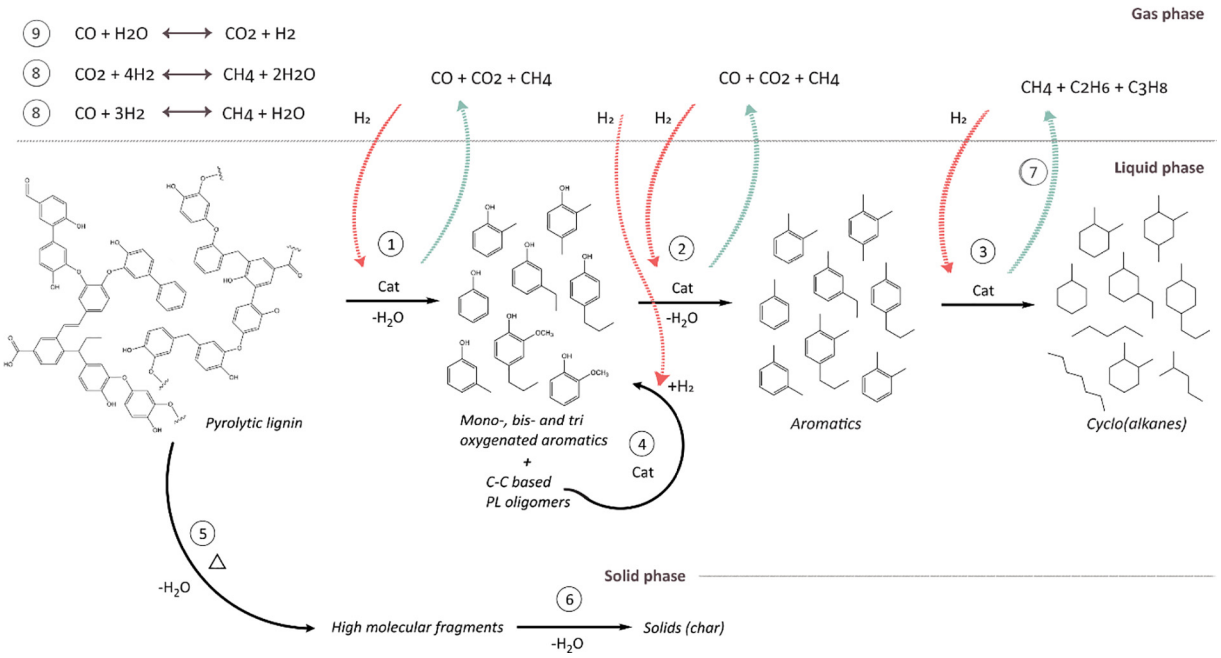

Fig. 13. Proposed global network for the catalytic hydrotreatment of PL.

lead to the production of gaseous alkanes such as ethane and propane (pathway 7), which were identified in amounts varying from 8 wt% (Pd/C) to 16 wt% ($NiMo/Al_2O_3$, Ru/C) in the product gas. Overall, noble-metal catalysts tend to favor the hydrogenation pathway, while sulphided catalysts yielded aromatics in higher proportions. As low molecular weight alkylphenolics and aromatics are important industrial chemicals of higher economic values in comparison with aliphatic fuel components, hydrogenation of the aromatic rings should be avoided. Overall, the products from noble metal catalysts presented higher monomer yields, and up to 19.1 wt% (based on PL intake) of the desired products (*i.e.* aromatics and alkylphenolics) were obtained with Pd/C, while the maximum yield achieved with $NiMo/Al_2O_3$ was 12.9 wt% (based on PL intake).

Oxygen removal was slightly more efficient for sulphided catalysts, as observed by the NMR analyses and elemental composition of the products, where sulphided catalysts showed a lower oxygen content of the products. During depolymerisation, also simultaneous decarbonylation, decarboxylation and demethylation reactions occur, *e.g.* removal of methoxy side groups. Gaseous products derived from hydrodeoxygenation and C—C cleavage reactions (mostly CO, CO_2 and CH_4) may further react with H_2 (methanation reactions, pathway 8) and H_2O (water-gas shift reaction, pathway 9). Such reactions are strongly dependent on the temperature, and conditions favoring further consumption of H_2 are undesired due to the high costs associated with it.

4. Conclusions

The catalytic hydrotreatment of a pine-derived PL to low molecular weight value-added products was investigated with a range of heterogeneous sulphided and non-sulphided catalysts. The best results were obtained with Pd/C, which showed high organic liquid yields and low amounts of gas phase products and solids formation. For this catalyst, almost 60 wt% of the organic product (*i.e.* 33 wt% based on PL intake) were monomers, as detected by GC analyses. The GC-detectable fraction consisted mostly of phenolics, aromatics and (cyclic) alkanes. The maximum yield of desired compounds (*i.e.* aromatics and alkylphenolics) was 19.1 wt% and 12.9 wt% for Pd/C and $NiMo/Al_2O_3$, respectively (amounts based on PL intake and obtained at 400 °C). The overall hydrocracking efficiency and gas yields were shown to be strongly dependent on the reaction temperature. Of interest is the observation that the product oil obtained with $NiMo/Al_2O_3$ contain higher amounts of aromatics compared to the noble metal catalysts. More remarkably is the observation that the aromatic content increases with reaction temperature for this catalyst and implies the occurrence of dehydrogenation reactions for this catalytic system.

As such, we conclude that the PL fraction from fast pyrolysis oils is an attractive feed for the synthesis of important biobased building blocks and products such as phenolic polymer precursors, fuel additives and phenol-based resins (*e.g.* phenol-formaldehyde). The promising results here reported are expected to have a positive effect on the techno-economic evaluation of pyrolysis liquids biorefineries. Further catalyst screening and characterization, as well as process optimization studies are required to improve the overall efficiency and product yields. A major challenge involves the development of efficient separation techniques for the various product classes. The successful separation of phenolics and hydrocarbons from hydrotreated pyrolysis oil was recently demonstrated at small-scale [44] by liquid-liquid extraction, indicating that technologies are available for this task.

Acknowledgements

Part of the work presented was conducted in the Lignin2Fuel project. The TKI Biobased Economy and the Netherlands Enterprise Agency (RVO) are gratefully acknowledged for their financial support of the Lignin2Fuel project under agreement no. TEBE116143. Financial support from the Science Without Borders program (Brazil) is gratefully acknowledged. We also thank Erwin Wilbers, Marcel de Vries, Léon Rohrbach, Jan Henk Marsman and Anne Appeldoorn for technical support and BTG for supplying pyrolytic lignin. Hans van der Velde is acknowledged for performing the elemental analyses, and Gert ten Brink is acknowledged for performing SEM analyses.

Appendix A. Supplementary data

Supplementary data to this article can be found online at https://doi.org/10.1016/j.fuproc.2019.02.020.

References

[1] A. Faaij, Modern biomass conversion technologies, Mitig. Adapt. Strateg. Glob.

Chang. 11 (2006) 343–375.
[2] A.V. Bridgwater, Renewable fuels and chemicals by thermal processing of biomass, Chem. Eng. J. 91 (2003) 87–102.
[3] S. Czernik, A.V. Bridgwater, Overview of applications of biomass fast pyrolysis oil, Energy Fuel 18 (2004) 590–598.
[4] A. Oasmaa, E. Kuoppala, Y. Solantausta, Fast pyrolysis of forestry residue. 2. Physicochemical composition of product liquid, Energy Fuel 17 (2003) 433–443.
[5] B. Scholze, C. Hanser, D. Meier, Characterization of the water-insoluble fraction from fast pyrolysis liquids (pyrolytic lignin): part II. GPC, carbonyl groups, and ^{13}C-NMR, J. Anal. Appl. Pyrolysis 58 (2001) 387–400.
[6] D.C. Elliott, Historical developments in hydroprocessing bio-oils, Energy Fuel 21 (2007) 1792–1815.
[7] R.H. Venderbosch, A.R. Ardiyanti, J. Wildschut, A. Oasmaa, H.J. Heeres, Stabilization of biomass-derived pyrolysis oils, J. Chem. Technol. Biotechnol. 85 (2010) 674–686.
[8] P. Grange, E. Laurent, R. Maggi, A. Centeno, B. Delmon, Hydrotreatment of pyrolysis oils from biomass: reactivity of the various categories of oxygenated compounds and preliminary techno-economical study, Catal. Today 29 (1996) 297–301.
[9] D.C. Elliott, T.R. Hart, G.G. Neuenschwander, L.J. Rotness, M.V. Olarte, A.H. Zacher, et al., Catalytic hydroprocessing of fast pyrolysis bio-oil from pine sawdust, Energy Fuel 26 (2012) 3891–3896.
[10] D.C. Elliott, T.R. Hart, G.G. Neuenschwander, L.J. Rotness, A.H. Zacher, Catalytic hydroprocessing of biomass fast pyrolysis bio-oil to produce hydrocarbon products, Environ. Prog. Sustain. Energy 28 (2009) 441–449.
[11] W. Yin, A. Kloekhorst, R.H. Venderbosch, M.V. Bykova, S.A. Khromova, V.A. Yakovlev, et al., Catalytic hydrotreatment of fast pyrolysis liquids in batch and continuous set-ups using a bimetallic Ni–Cu catalyst with a high metal content, Catal. Sci. Technol. 6 (2016) 5899–5915.
[12] J. Wildschut, M. Iqbal, F.H. Mahfud, I. Mélian-Cabrera, R.H. Venderbosch, H.J. Heeres, Insights in the hydrotreatment of fast pyrolysis oil using a ruthenium on carbon catalyst, Energy Environ. Sci. 3 (2010) 962–970.
[13] A.R. Ardiyanti, S.A. Khromova, R.H. Venderbosch, V.A. Yakovlev, I.V. Melián-Cabrera, H.J. Heeres, Catalytic hydrotreatment of fast pyrolysis oil using bimetallic Ni–Cu catalysts on various supports, Appl. Catal. A Gen. 449 (2012) 121–130.
[14] J. Wildschut, I. Mélian-Cabrera, H.J. Heeres, Catalyst studies on the hydrotreatment of fast pyrolysis oil, Appl. Catal. B Environ. 99 (2010) 298–306.
[15] J. Wildschut, F.H. Mahfud, R.H. Venderbosch, H.J. Heeres, Hydrotreatment of fast pyrolysis oil using heterogeneous noble-metal catalysts, Ind. Eng. Chem. Res. 48 (2009) 10324–10334.
[16] J.D. Adjaye, R.K. Sharma, N.N. Bakhshi, Catalytic conversion of wood derived bio-oil to fuels and chemicals, Stud. Surf. Sci. Catal. 73 (1992) 301–308.
[17] R.K. Sharma, N.N. Bakhshi, Upgrading of pyrolytic lignin fraction of fast pyrolysis oil to hydrocarbon fuels over HZSM-5 in a dual reactor system, Fuel Process. Technol. 35 (1993) 201–218.
[18] J. Piskorz, P. Majerski, D. Radlein, D.S. Scott, Conversion of lignins to hydrocarbon fuels, Energy Fuel 3 (1989) 723–726.
[19] W. Chen, D.J. McClelland, A. Azarpira, J. Ralph, Z. Luo, G.W. Huber, Low temperature hydrogenation of pyrolytic lignin over Ru/TiO_2: 2D HSQC and ^{13}C NMR study of reactants and products, Green Chem. 18 (2016) 271–281.
[20] A. Kloekhorst, J. Wildschut, H.J. Heeres, Catalytic hydrotreatment of pyrolytic lignins to give alkylphenolics and aromatics using a supported Ru catalyst, Catal. Sci. Technol. 4 (2014) 2367–2377.
[21] Q. Zhang, J. Gong, M. Skwarczek, Y. Dajun, Y. Fengqi, Sustainable process design and synthesis of hydrocarbon biorefinery through fast pyrolysis and hydroprocessing, AICHE J. 60 (2014) 980–994.
[22] P. Panagiotopoulou, D.I. Kondarides, X.E. Verykios, Mechanistic study of the selective methanation of CO over Ru/TiO_2 catalyst: identification of active surface species and reaction pathways, J. Phys. Chem. C 115 (2011) 1220–1230.
[23] J.B. Bredenberg, M. Huuska, J. Räty, M. Korpio, Hydrogenolysis and hydrocracking of the carbon-oxygen bond: I. Hydrocracking of some simple aromatic O-compounds, J. Catal. 77 (1982) 242–247.
[24] R. Bayerbach, D. Meier, Characterization of the water-insoluble fraction from fast pyrolysis liquids (pyrolytic lignin). Part IV: structure elucidation of oligomeric molecules, J. Anal. Appl. Pyrolysis 85 (2009) 98–107.
[25] D.J. McClelland, A.H. Motagamwala, Y. Li, M.R. Rover, A.M. Wittrig, C. Wu, et al., Functionality and molecular weight distribution of red oak lignin before and after pyrolysis and hydrogenation, Green Chem. 19 (2017) 1378–1389.
[26] B. Scholze, D. Meier, Characterization of the water-insoluble fraction from pyrolysis oil (pyrolytic lignin). Part I. PY–GC/MS, FTIR, and functional groups, J. Anal. Appl. Pyrolysis 60 (2001) 41–54.
[27] Z. Tang, Y. Zhang, Q. Guo, Catalytic hydrocracking of pyrolytic lignin to liquid fuel in supercritical ethanol, Ind. Eng. Chem. Res. 49 (2010) 2040–2046.
[28] D.C. Elliott, T.R. Hart, Catalytic hydroprocessing of chemical models for bio-oil, Energy Fuel 23 (2009) 631–637.
[29] T. Prasomsri, M. Shetty, K. Murugappan, Y. Román-Leshkov, Insights into the catalytic activity and surface modification of MoO_3 during the hydrodeoxygenation of lignin-derived model compounds into aromatic hydrocarbons under low hydrogen pressures, Energy Environ. Sci. 7 (2014) 2660–2669.
[30] C.R. Lee, J.S. Yoon, Y. Suh, J. Choi, J. Ha, D.J. Suh, et al., Catalytic roles of metals and supports on hydrodeoxygenation of lignin monomer guaiacol, Catal. Commun. 17 (2012) 54–58.
[31] E. Laurent, C. Pierret, P. Grange, B. Delmon, Control of the deoxygenation of pyrolytic oils by hydrotreatment, Proc. of 6th Conference on Biomass for Energy, Industry and Environment, Athens, Greece, 1991, pp. 665–671.
[32] C. Leyva, J. Ancheyta, G. Centeno, Effect of alumina and silica–alumina supported NiMo catalysts on the properties of asphaltenes during hydroprocessing of heavy petroleum, Fuel. 138 (2014) 111–117.
[33] N. Kagami, B.M. Vogelaar, A.D. van Langeveld, J.A. Moulijn, Reaction pathways on $NiMo/Al_2O_3$ catalysts for hydrodesulfurization of diesel fuel, Appl. Catal. A Gen. 293 (2005) 11–23.
[34] V. LaVopa, C.N. Satterfield, Catalytic hydrodeoxygenation of dibenzofuran, Energy Fuel 1 (1987) 323–331.
[35] O. Şenol, E. Ryymin, T. Viljava, A. Krause, Reactions of methyl heptanoate hydrodeoxygenation on sulphided catalysts, J. Mol. Catal. A Chem. 268 (2007) 1–8.
[36] E. Laurent, B. Delmon, Study of the hydrodeoxygenation of carbonyl, carbocylic and guaiacyl groups over sulfided CoMo/γ-Al_2O_3 and NiMo/γ-Al_2O_3 catalysts: I. Catalytic reaction schemes, Appl. Catal. A Gen. 109 (1994) 77–96.
[37] S. Bezergianni, A. Dimitriadis, G. Meletidis, Effectiveness of CoMo and NiMo catalysts on co-hydroprocessing of heavy atmospheric gas oil–waste cooking oil mixtures, Fuel. 125 (2014) 129–136.
[38] C.R. Kumar, N. Anand, A. Kloekhorst, C. Cannilla, G. Bonura, F. Frusteri, et al., Solvent free depolymerization of Kraft lignin to alkyl-phenolics using supported NiMo and CoMo catalysts, Green Chem. 17 (2015) 4921–4930.
[39] N. Labbé, T.G. Rials, S.S. Kelley, Z. Cheng, J. Kim, Y. Li, FT-IR imaging and pyrolysis-molecular beam mass spectrometry: new tools to investigate wood tissues, Wood Sci. Technol. 39 (2005) 61–76.
[40] M. Liu, A. Baum, J. Odermatt, J. Berger, L. Yu, B. Zeuner, et al., Oxidation of lignin in hemp fibres by laccase: effects on mechanical properties of hemp fibres and unidirectional fibre/epoxy composites, Compos. A: Appl. Sci. Manuf. 95 (2017) 377–387.
[41] P. Moyer, K. Kim, N. Abdoulmoumine, S.C. Chmely, B.K. Long, D.J. Carrier, et al., Structural changes in lignocellulosic biomass during activation with ionic liquids comprising 3-methylimidazolium cations and carboxylate anions, Biotechnol. Biofuels 11 (2018) 265.
[42] L.M. Aguilera-Sáez, F.M. Arrabal-Campos, Á.J. Callejón-Ferre, M.D.S. Medina, I. Fernández, Use of multivariate NMR analysis in the content prediction of hemicellulose, cellulose and lignin in greenhouse crop residues, Phytochemistry 158 (2019) 110–119.
[43] C.G. Boeriu, D. Bravo, R.J. Gosselink, J.E. van Dam, Characterisation of structure-dependent functional properties of lignin with infrared spectroscopy, Ind. Crop. Prod. 20 (2004) 205–218.
[44] Z. Cao, J. Engelhardt, M. Dierks, M.T. Clough, G. Wang, E. Heracleous, et al., Catalysis meets nonthermal separation for the production of (alkyl) phenols and hydrocarbons from pyrolysis oil, Angew. Chem. 129 (2017) 2374–2379.